International Journal of Advanced Chemistry, 7 (1) (2019) 67-72

International Journal of Advanced Chemistry

Website: www.sciencepubco.com/index.php/IJAC

Research paper

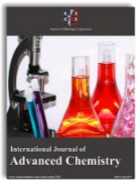

Synthesis, characterization and DFT studies of a palladium (ii) complex with bidentate Schiff base ligands

Surajit Chakrabarty [1] *, Shoumik Bhattacharjee [2], Rachida Rahmani [3], Afzal Hussain Sheikh [4], Abdelkader Chouaih [3] *, Fodil Hamzaoui [5]

[1] Department of Chemistry, Government Degree College, Dharmanagar, North Tripura - 799250, India
[2] Department of Chemistry, Ledrai Dewan Class XII School, Machmara, Unakoti ,Tripura-799263, India
[3] LTPS Laboratory, Abdelhamid Ibn Badis University of Mostaganem, 27000 Mostaganem, Algeria
[4] Department of Chemistry, N.C College, Badarpur, Karimgang, Assam-788806, India
[5] LPFM Académie de Montpellier – France
**Corresponding author E-mail: achouaih@gmail.com*

Abstract

The N-donor bidentate complexes of Palladium (II) of the type [PdL1Cl2] and [PdL2Cl2] {where L1 = N, N'-bis(napthanidal)-1,4-diacetyldihydiimine and L2= N, N'-bis(napthanidal)-1,2-ethylenediimine} were synthesized by refluxing of PdCl2 in acetonitrile with ligand L1 and L2. Complexes have been characterized by elemental analysis, conductivity measurement, IR, UV-Vis and 1H-NMR spectroscopy. Full geometry optimization of the ground state of the complex [PdL1Cl2] was carried out using Density Functional Theory (DFT) at B3LYP functional with 6-311G(d, p) basis set for C, N, Cl, H and LANL2DZ basis set for Pd atoms in gas and solvent (DMSO) phases. The calculated geometric and spectral results reproduced the experimental data with well agreement. Theo-retical calculated molecular orbitals (HOMO–LUMO) and their energies have been calculated that suggest charge transfer occurs within the complexes. The HOMO-LUMO energy gap was found 2.6210 eV. The electrophilic and nucleophilic sites are theoretically evaluated by molecular electrostatic potential.

Keywords: *Pd (II); Bidentate; IR; UV-Vis; 1H-NMR; DFT.*

1. Introduction

The Chemistry of metal complexes with Schiff base ligands has vital role in the biological field due to their well known antifungal and antibacterial activity (Garoufis et al. 2009, Mukherjee et al. 2011, Abdel Ghani et al. 2001). Considerable interest has been given to transition metal complexes with Schiff base ligands on account of their structural diversity, stability, ease of preparation and variety of applications (Pal et al. 2000, De et al. 2011, Tong et al. 2014). The coordination chemistry of square planner Pd(II) with N-donor Schiff base ligands and their DFT studies have gain importance due to their antitumor , anticancer and catalytic activities (Akbari et al. 2013, Sönmez et al. 2010, Mocanu et al. 2010, Anan et al. 2011, Petrović et al. 2015).

In view of diverse chemistry possessed by the Pd (II) Schiff base complexes, we under took the synthesis and characterization of Pd (II) complexes containing bidentate N-donor ligands L1 and L2. Structural elucidation of [PdL1Cl_2] was carried out using Density Functional Theory (DFT) which exhibit slightly distorted square planar arrangement around the Pd (II) metal center ((Ruike et al. 1996, Akbari et al. 2013). Schiff base bidentate N-donor ligands viz. N, N'-bis(napthanidal)-1,4-diacetyldihydiimine (L1) and L2= N, N'-bis(napthanidal)-1,2-ethylenediimine (L2) (Fig. 1) were prepared according to or similar to the reported methods earlier (Busch et al. 1956, Bariz et al. 1986, Hauer et al. 1987, Kesslen et al. 1995, Pal et al. 2000, Chowdhury et al. 2003).

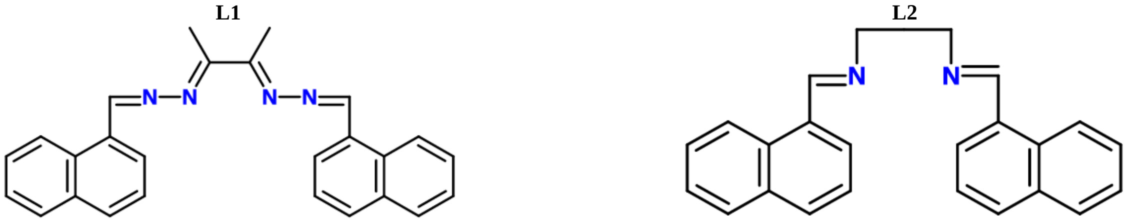

Fig. 1: Structure of Bidentate N-Donor Ligands L1 & L2, Where L1= N, N'-Bis (Napthanidal)-1,4-Diacetyldihydiimine and L2= N, N'-Bis (Napthanidal)-1, 2-Ethylenediimine.

2. Experimental

All chemicals used were of AR or chemically pure grade. Solvents were purified prior to use by standard methods. Diacetely (2,4-butanedione), 1-Napthaldhyde ethylenediamine and $PdCl_2$ were purchased from Merck. Molar conductivity measurements of millimolar dimethylsulphoxide (DMSO) solutions were made on a Wayne-Kerr Automatic Precision B905 conductometer. IR spectra were recorded as KBr pellets using a Perkin-Elmer 983 or 410 Nicolet spectrophotometer. C, H and N analyses were carried out at SAIF, NEHU, Shillong. Spectroscopic grade solvents were used for cyclic voltammetry and UV–Vis measurements. UV–Vis spectra were recorded on a Beckman DU 650 spectrophotometer in DMSO. Cyclic voltammetry experiments were recorded on a CH instruments electrochemical analyzer CHI 620B under nitrogen. Magnetic susceptibility measurements at room temperature were carried out on a Sherwood Scientific magnetic susceptibility balance.

2.1. Preparation of [PdLCl2] (where L=L1 & L2)

Pd (II) complexes with Schiff bases were synthesized by refluxing of $PdCl_2$ (0.18g, 1mmol) in acetonitrile (25 cm^3) for 0.5 h to get clear solution. When a clear solution was obtained, ligand L (L=L1 & L2) was added and continued for reflux for another 4h. On standing at room temperature, a compound was separated out which was isolated by centrifugation and washed with diethyl ether and dried in vacuo, yielded a complex of the composition [$PdLCl_2$]. The yield was recorded for both the complexes (~ 75%).

3. Theoretical investigation

All calculations were performed within Gaussian 09 program package (Frisch et al. 2009). The Gauss-View molecular visualization software (Frisch et al. 2009) was used for post-processing. Full geometry optimization of the ground state complexes was carried out using density functional theory (DFT) at B3LYP (Becke et al. 1993, Lee et al. 1988) functional in gas and solvent (DMSO) phases with 6-311G(d, p) basis set for C, N, Cl, H and LANL2DZ for Pd atoms.

4. Results and discussion

4.1. Experimental spectroscopic analysis

A reaction of $PdCl_2$ with bidentate ligand in acetronitrile yielded [$PdLCl_2$] (Where L=L1 & L2). These compounds are air stable and insoluble in most of the organic solvents but soluble in dimethylsulphoxide, and N, N'-dimethylformamide. The micro analytical data (Table 1) are in conformity with the composition [$PdLCl_2$]. Conductivity measurements in milimolar solution of these complexes in DMSO solution showed molar conductance values in the range 12-17 Ohm^{-1} cm^2 mol^{-1} confirming the covalent nature of the chloro groups (Geary et al. 1987). The Schiff base ligands are characterized by infrared and ^1H NMR spectra with the reported ones (Bariz et al. 1986, Hauer et al. 1987, Kesslen et al. 1995, Chowdhury et al. 2003, De et al. 2011). IR and ^1H NMR spectral data of the Schiff base ligands and their complexes with Pd(II) are presented in Table 2. Magnetic susceptibility measurements show that complexes are diamagnetic, thereby confirming low spin Pd(II), d^8 configuration. Infrared spectra of free Schiff base ligands L (Where L=L1 & L2) show very strong absorption bands at 1600 and 1631 cm^{-1} which are assigned to $\nu_{C=N}$ of the azomethine group. In complex [$PdL1Cl_2$], non shifting of this absorption band indicates that Pd(II) metal atom is not coordinated with the azomethine N-atom ,while in [$PdL2Cl_2$] this band has been shifted at 1646 cm^{-1}, indicating the coordination of the Schiff base ligand with metal atom through azomethine N-atom (Busch et al. 1956, Bariz et al. 1986, Hauer et al. 1987, Kesslen et al. 1995, Chowdhury et al. 2003). In [$PdL1Cl_2$] complex, shifting of N-N stretching frequency to higher wave number (1228 cm^{-1}) as compare to the free ligand (1129 cm^{-1}) , indicates one of the N-atom (other than the azomethine N-atom) is co-ordinated to Pd(II) metal ion. Besides these bands, all other characteristic vibrations are also observed in both the complexes. Electronic absorption spectra of [$PdL1Cl_2$] complex in dimethylsulphoxide {(Table 2 and Fig. 2 (a & b)} shows two bands at 460 and 520 nm with ε in the order of 10^3. These bands may be assigned to the charge transfer type of transition arising from the filled d-orbital of Pd (II) to the vacant π^* orbital of Schiff base ligand. Bands in the region 345-400 nm are also observed for both the complexes which may be assigned to the intra-ligands transition of the type $n\rightarrow \pi^*$ or $\pi\rightarrow \pi^*$. Further in case of [$PdL1Cl_2$] one broad band at 737 nm is also observed which may be assigned to the d-d transition of the type $^1A_{1g}\rightarrow {}^1B_{1g}$ or $^1A_{1g}\rightarrow {}^1A_{2g}$ (Lever 1984, Chakrabarty et al. 2010, Chakrabarty et al. 2014).

The cyclic voltammetric studies in dimethylsulphoxide in presence of TBAP showed viz. [$PdLCl_2$] (where L= L1,& L2) one quasi-reversible couple in the range +0.02V to +0.15V which may be assigned to the Pd^{IV}/Pd^{II} couple, whereas in case of [$PdL2Cl_2$], one irreversible oxidation is observed at +0.45V (Chakrabarty et al. 2010).

^1H NMR spectra of [$PdL1Cl_2$] and [$PdL2Cl_2$] showed multiplets in the region of δ 7.35 – δ9.0 which could be attributed to the aromatic protons due to naphthalene group. Doublet at δ 2.35 and singlet at δ 4.30 were observed for the two complexes due to the presence of two methyl groups in [$PdL1Cl_2$] and two methelene groups in [$PdL2Cl_2$]. Signals due to -CH=N proton were observed at δ 9.50 and δ 9.95 for the complexes with L1 and L2 ligands respectively. The shifting of azomethine proton signal by δ 0.98 in the complex with L2 compared to the corresponding free ligand in ^1H NMR spectra, indicates the coordination of the Schiff base ligand with metal atom through azomethine N-atom as predicted from IR spectra explained earlier (Busch et al. 1956, Hauer et al. 1987, Kesslen et al. 1995, Chowdhury et al. 2003, De et al. 2011).Signal due to -CH=N protons in [$PdL1Cl_2$] is observed as singlet at δ9.5 which is almost equal to the signal in the free ligand δ9.49, that indicates azomethine N-atom is not bonded with the metal ion as predicted from IR spectroscopy also.

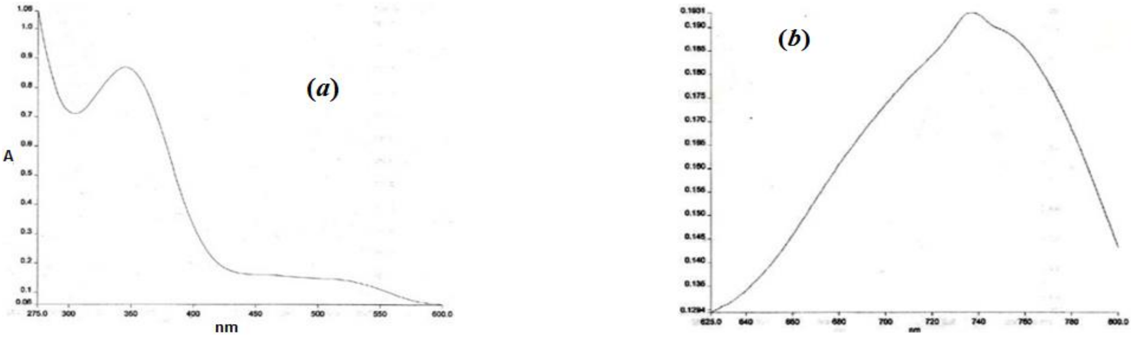

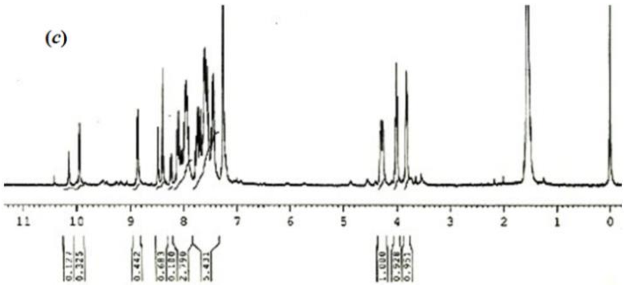

Fig. 2: (A) And (B) Electronic Absorption Spectra of [Pdl1cl$_2$] in DMSO, (C) ^{1}H NMR Spectrum of [Pdl2cl$_2$] in DMSO-D$_6$.

Table 1: UV-Vis Results Recorded in DMSO. Calculated Values are in Parenthesis

Complex	Color	Melting point °C	Elemental Analysis (%)^a			UV-Vis (λ_{max}) (nm)
			C	H	N	
[PdL1Cl2]	Brown	>340	54.78 (55.03)	3.60 (3.88)	9.65 (9.88)	737 (3.04x10^2), 520 (4.41x 10^3), 460 (5.05x 10^3), 345 (2.74x 10^4)
[PdL2Cl2]	Chocolate Brown	330	55.70 (56.14)	4.20 (3.90)	6.00 (5.45)	394 (1.36x 10^4), 372 (1.33x 10^4)

Table 2: Experimental IR and ^{1}H NMR Spectral Data of the Schiff Base Ligands and Their Complexes with Pd (II)

Ligand/ Complex	IR	^{1}H-NMR
L1	$\nu_{as(C\text{-}H)}$ 3045; $\nu_{s(C\text{-}H)}$ 2899; $\nu_{(C=N)}$ 1600; $\delta_{as(C\text{-}CH)}$ 1520, 1434; $\delta_{s(C\text{-}CH)}$ 1348 ;$\nu_{(N\text{-}N)}$ 1129	2.154,2.48 (d, CH$_3$), 7.40-9.0 (m, aromatic), 9.49 (d, CH=N)
[PdL1Cl2]	$\nu_{as(C\text{-}H)}$ 3045, 2919 ; $\nu_{s(C\text{-}H)}$ 2866 ; $\nu_{(CH=N)}$ 1600; $\delta_{as(C\text{-}CH)}$ 1574, 1374, 1341; $\delta_{s(C\text{-}CH)}$ 1434; $\nu_{(N\text{-}N)}$ 1228	2.35 (d-CH$_3$), 7.35-8.35 (m, aromatic) 9.5 (d, CH=N)
L2	$\nu_{as(C\text{-}H)}$ 3048; $\nu_{s(C\text{-}H)}$ 2898; $\nu_{(C=N)}$ 1631; ν (aromatic)1337,1238	4.20(s, CH$_3$), 7.35-8.80 (m, aromatic), 8.97(s, CH=N)
[PdL2Cl2]	$\nu_{as(C\text{-}H)}$ 3071,2945; $\nu_{(CH=N)}$ 1646; $\delta_{as(C\text{-}CH)}$ 1447; $\delta_{s(C\text{-}CH)}$ 1361;	4.30 (s, CH$_2$), 7.4-9.0 (m, aromatic), 9.95 (d, CH=N)

Abbreviations N = Stretching Δ = Deformation, S = Symmetric and As = Antisymmetric.

4.2. DFT structural assignment for [PdL1Cl2]

DFT structural analysis of [PdL1Cl$_2$] complex was performed using B3LYP functional in gas and solvent (DMSO) phases with 6-311G(d, p) basis set for C, N, Cl, H and LANL2DZ for Pd atoms, which indicates the slightly distorted square planar geometry of the complex around Pd (II) metal center with strong evidence of bond length similar to the reported elsewhere (Busch et al. 1956, Hauer et al. 1987, Ruike et al. 1996, Frisch et al. 2009, Akbari et al. 2013). The optimized structure of [PdL1Cl$_2$] is illustrated in Fig. 3(a) and the corresponding main geometrical parameters (bonds lengths and bond angles) are listed in Table 3 as we can see there is a good agreement between the calculated and the experimental values (Bariz et al. 1986, Hauer et al. 1987, Kesslen et al. 1995, Pal et al. 2000). N$_1$-N$_2$ and N$_3$-N$_4$ bond distances in the complex [PdL1Cl$_2$] are lower than that of the free ligand (1.387 Å) that indicates the coordination of N$_1$ and N$_3$ with Pd (II) metal ion. This statement has also good accord with the prediction of IR and ^{1}H-NMR spectroscopy. The bond lengths Pd-N$_1$ and Pd-N$_3$ of the complex are 2.105Å & 2.097Å, respectively implying the presence of regular and dative bonding. The difference between the experimental and calculated bond lengths obtained at 6-311G(d, p) basis set does not exceed 0.072Å (Pd-N$_3$),whereas in the case of 6-311G(d, p) DMSO with same basis set , the largest difference between the observed and the calculated values is about 0.064 Å . The bond angles for 6-311G(d, p) DMSO calculations are very close the experimental value and the maximum difference is about 2.51°. For DFT with 6-311G(d, p) basis the bond angle difference does not exceed 2.73°. The dihedral angles Pd-N1-N2-C3 and Pd-N3-N4-C16 (about 40°) indicate that the fragment (Cl1, Pd, Cl2) is not in the same plane with the rest of the complex. In summary, the optimized geometrical parameters obtained using the DFT method are in good agreement with the corresponding literature results. It is worth noting that some of the optimized bond angles and bond lengths have slightly different values from the corresponding experimental ones, due to the fact that the theoretical calculations consider only isolated molecules in the gaseous phase while the experimental results refer to molecules in the crystal environment.

4.3. HOMO-LUMO and MEP calculation

The HUMO-LUMO energies of the complex are calculated to be -5.8668 eV and -3.2458 eV respectively, where ΔE = 2.6210 eV matched well those reported to similar Pd(II) complexes with Schiff base. Dipole moment of the complex [PdL1Cl$_2$], is calculated as 9.6 D in the XY plane, which indicates that all electronegative atoms are located within the square plane (Akbari et al. 2013).

It is well known that molecular electrostatic potential (MEP) provides a visual method to understand the reactivity of the molecules and correlates with dipole moment (Drissi et al. 2015). The MEP values can be determined experimentally by X-ray diffraction or by computational methods (Boubegra et al. 2016, Benaissi et al. 2018, Boukabcha et al. 2018). MEP of the complex is computed using B3LYP/6-311G(d,p) optimized geometry and its surface map is shown in Fig. 3(b). This map shows that the electrophilic region (red) is located on the Chlorine atoms, while the nucleophilic region (blue) is located over the hydrogen atoms.

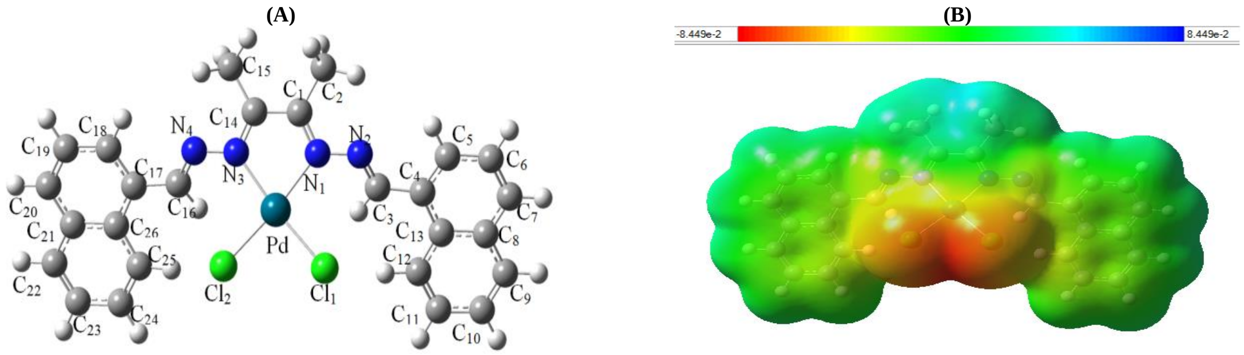

Fig. 3: [Pdl1cl$_2$]: (A) Optimized Ground State Structure in Gas Phase as Obtained from DFT and (B) Molecular Electrostatic Potential Map.

4.4. Theoretical spectroscopic analysis

The IR spectrum based on the theoretically predicted wavenumbers by B3LYP/6-311G(d,p) level with DMSO solvent is shown in Fig. 5 and the corresponding assignments are depicted in Table 4. No negative frequency has been found, which means that the optimized geometry is located at the local lowest point on the potential energy surface. The calculated frequencies are higher than the experimental values for the majority of the normal modes, for this reason the scaling factors 0.967 is used for calculated frequencies (Pulay et al. 1983, Johnson et al. 2013).

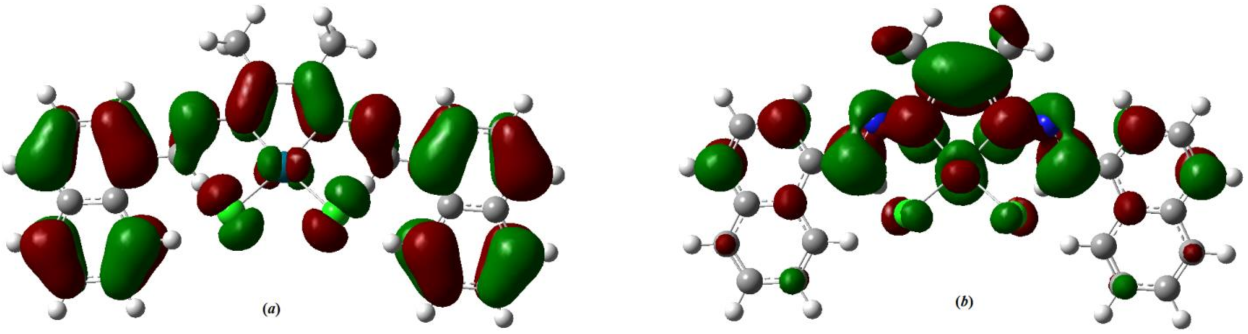

Fig. 4: HOMO and LUMO Plots: (A) HOMO (B) LUMO.

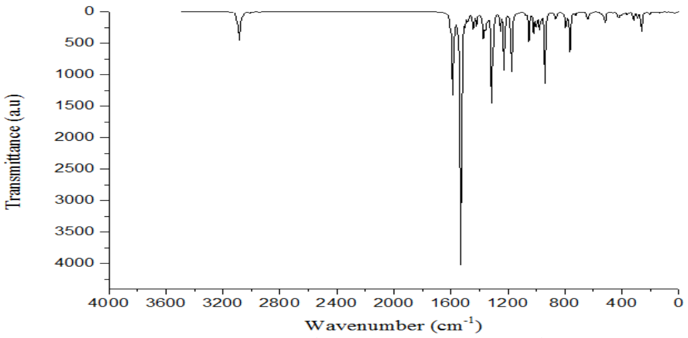

Fig. 5: The Calculated Scaled Infrared Vibrational Spectrum of [Pdl1cl2].

The theoretical ^{1}H isotropic shielding is computed with B3LYP/ 6-311G (d,p) level using the gauge-independent atomic orbital (GIAO) method (Wolinski et al. 1990) with DMSO solvent and the results are shown in Table 4. To calculate the chemical shift for the title compound, a geometry optimization and NMR spectrum of the TMS has been computed with the same level of theory. From that, the TMS shielding with B3LYP/GIAO/6-311G(d,p) with DMSO is 31.998 ppm for ^{1}H NMR. Numerical values of chemical shift □□$_{\text{□PdL1Cl2□□}}$□□σ $_{\text{□TMS□}}$□– σ $_{\text{□PdL1Cl2□□}}$where δ : chemical shift and σ : chemical shielding (Bohmann et al. 1997). As it can be observed from Table 4, chemical shift is in good agreement with the experimental ^{1}H NMR results (Table 2). Thus the results show that the B3LYP functional with GIAO method and 6-311G (d, p) basis set with DMSO solvent predicted well the ^{1}H NMR spectrum.

Table 3: Selected Optimized Bond Lengths and Bond Angles of Pd in Gas Phase and Solution Phase Computed at B3LYP Method with 6–311G (D, P) Basis Set

Bond length (Å)	B3LYP/6-311G (d,p)	B3LYP/6-311G (d,p)/DMSO	Exp.	Bond Angle (°)	B3LYP/6-311G (d,p)	B3LYP/6-311G (d,p)/DMSO	Exp.
Pd–N1	2.105	2.083	2.065	N1–Pd–Cl2	173.07	173.19	178.2
Pd–N3	2.097	2.079	2.025	N3–Pd–Cl1	173.34	173.02	177.2
Pd–Cl1	2.343	2.388	2.324	Pd–N1–C1	113.51	114.06	111.55
Pd–Cl2	2.342	2.388	2.324	Cl1–Pd–Cl2	88.58	88.54	89.52
N1–N2	1.366	1.369	1.413	Cl1–Pd–N1	96.96	96.76	94.3
N3–N4	1.364	1.367	1.411	Cl2–Pd–N3	96.69	96.61	96.58
N1–C1	1.311	1.307	1.291	N1–Pd–N3	77.49	77.76	80.22

Table 4: Calculated Wavenumbers IR and ^{1}H-NMR Data for the Title Complex

Complex	IR (B3LYP/6-311G(d,p)	1H-NMR/ GIAO/B3LYP/6-311G(d,p)
[PdL1Cl2]	$\nu_{as(C-H)}$ 3087-2993 ; $\nu_{s(C-H)}$ 2943 ; $\nu_{(CH=N)}$ 1585; $\delta_{as(C-CH\ )}$ 1529, 1368, 1314; $\delta_{s(C-CH\ )}$ 1444; $\nu_{(N-N)}$ 1174	2.12-3,59 (CH_3), 8.0-9.1(m, aromatic) 9.7 (d, CH=N)

Table 5: The Calculated Thermodynamic Parameters of the Title Complex Using B3LYP Functional with 6-311G (D, P) Basis Set at Different Temperatures

B3LYP/6-311G(d,p)			- ΔG (KJ/mole)	lnK$_s$
T(K)	ΔS (J/mol.K)	ΔH (KJ/mol)		
100	504.71	13.31	37.16	44.70
200	701.34	42.51	97.76	58.79
298.2	873.88	85.4	175.15	70.66
300	877.04	86.34	176.77	70.87
400	1043.07	144.38	272.85	82.04
500	1199.74	214.8	385.07	92.63
600	1346.23	295.28	512.46	102.73
700	1482.55	383.81	653.98	112.37
800	1609.34	478.82	808.65	121.58
900	1727.45	579.15	975.56	130.38
1000	1837.77	683.89	1153.88	138.79

4.5. Effect of temperature

The degree of formation of complex [$PdL1Cl_2$] , was obtained from the relation given below that varies with thermodynamic parameters of the metal ion complex at different temperatures using Density Functional Theory (DFT) at B3LYP functional with 6-311G(d, p) basis set for C, N, Cl, H and LANL2DZ for Pd atoms. From the curve (Fig 6), it is clear that the stability constant (K_s) value increases with the increase of temperature that means the complex formation reaction is endothermic in nature. Thus rise in temperature is favorable for the formation of stable complex. The complex formation is a spontaneous process and the spontaneity increases with temperature.

$\Delta G = - RT \ln K_s$; $\ln K_s = -\Delta H/RT + \Delta S/R$, where ΔG= Change in Gibbs free Energy , K_s = Stability Constant , ΔS= Change in entropy , ΔH = Change in Enthalpy , R is universal gas constant and T is temperature in Kelvin.

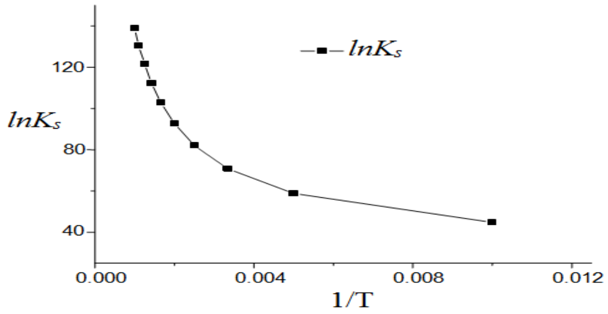

Fig. 6: Effect of Temperature on Lnk_s.

5. Conclusion

Complexes of Palladium (II) with N-donor Schiff base ligands viz [$PdL1Cl_2$] and [$PdL2Cl_2$], have been synthesized. The DFT structural study for the complex [$PdL1Cl_2$] was carried out by using Density Functional Theory (DFT) at B3LYP functional with 6-311G (d, p) basis set for C, N, Cl, H and LANL2DZ for Pd atoms in gas and solvent (DMSO) phases. Thus from DFT analysis, the structure of [$PdL1Cl_2$] complex has been proposed to be slightly distorted square planar geometry confirmed by the dihedral angles Pd-N-N-C (about 40°). The other complex [$PdL2Cl_2$] also possesses slightly distorted square planar geometry which can be proposed on the basis of physical and analytical observations. The HOMO-LUMO energy gap and the molecular electrostatic potential are discussed.

Acknowledgments

One of the Authors, S. Chakrabarty is thankful to the Head SAIF, North Eastern Hill University, Shillong for CHN analysis and spectral studies and also to Dr. Sambhunath Rakshit, Principal, Government Degree College, Dharmanagar, for allowing to carry out the research work in the Department of Chemistry, Government Degree College, Dharmanagar. Financial support under MRP Scheme (Sanction No. F.5-332/2015-16/MRP/NERO/1114, dated 29.03.2016) from the UGC-NERO, Assam, India is gratefully acknowledged. S. Chakrabarty is also grateful to Dr. Aziz Ahmed, Department of Chemistry, Indian Institute of Technology, Patna-18, Bihar India for his helpful discussion. Mahmood U, Kaul VK, Acharya R, Jerovetz L. p-Coumaric acid esters from, Tanacetum longifolium. Phytochemistry, 2003; 64(4): 851-853. (For Article)

References

[1] Garoufis A, Hadjikakou SK & Hadiliadis N (2009), Palladium coordination compounds as anti-viral, anti-fungal, anti-microbial and anti-tumor agents. *Coordination Chemistry Reviews* 253, 1384–1397. https://doi.org/10.1016/j.ccr.2008.09.011.

[2] Mukherjee S, Chowdhury S, Chattapadhyay AP & Bhattacharya A (2011), Spectroscopic, cytotoxic and DFT studies of a luminescent palladium (II) complex of a hydrazone ligand that induces apoptosis in human prostate cancer cells. *Inorganica Chimica Acta* 373, 40–46. https://doi.org/10.1016/j.ica.2011.03.048.

[3] Abdel Ghani NT & Mansour AM (2011), Novel Pd(II) and Pt(II) complexes of N,N-donor benzimidazole ligand: Synthesis, spectral, electrochemical, DFT studies and evaluation of biological activity. *Inorganica Chimica Acta* 373, 249–258. https://doi.org/10.1016/j.ica.2011.04.036.

[4] Pal PK, Chowdhury S, Drew MGB & Datta D (2000), Metal-assisted electrocyclic reaction in a C=N–N=C–C=N system. *New Journal of Chemistry* 24, 931–933. https://doi.org/10.1039/b006547l.

[5] Pal PK, Chowdhury S, Purkayastha P, Tocher DA & Datta D (2000), A novel double-stranded dinuclear copper(I) helicate having a photoluminescent CuI2N8 chromophore. *Inorganic Chemistry Communications* 3, 585–589. https://doi.org/10.1016/S1387-7003(00)00147-7.

[6] De S, Chowdhury S, Drew MGB & Datta D (2011), Effect of an ancillary ligand on single helix-double helix interconversion in copper complexes. Copper(I)-water bond. *Indian Journal of Chemistry - Section A* 50, 171–175. http://nopr.niscair.res.in/handle/123456789/11016

[7] Tong GSM, Chow PK, To WP, Kwok W-M & Che CM (2014), A Theoretical Investigation into the Luminescent Properties of d^8-Transition-Metal Complexes with Tetradentate Schiff Base Ligands. *Chemistry–A European Journal* 20, 6433–6443. https://doi.org/10.1002/chem.201304375.

[8] Akbari A & Bakhte-ei Z (2013), Synthesis, Experimental and Theoretical Characterization of Bidentate 5-Nitro-2-(Pyridin-2-Yl)-1H-Benzo[D] Imidazole Ligand and its Pd (II) Complex. *Computational Research* 1, 85–90. https://doi.org/10.13189/cr.2013.010303

[9] Anan NA, Hassan SM, Saad EM, Butler IS & Mostafa SI (2011), Preparation, characterization and pH-metric measurements of 4-hydroxysalicylidenechitosan Schiff-base complexes of Fe(III), Co(II), Ni(II), Cu(II), Zn(II), Ru(III), Rh(III), Pd(II) and Au(III). *Carbohydrate Research* 346, 775–793. https://doi.org/10.1016/j.carres.2011.01.014.

[10] Petrović VP, Živanović MN, Simijonović D, Đorović J, Petrović ZD & Markovićb SD (2015), Chelate N, O-palladium (II) complexes: synthesis, characterization and biological activity. *RSC Advances* 5, 86274–86281. https://doi.org/10.1039/C5RA10204A.

[11] Sönmez M, Çelebi M, Yardım Y & Şentürk Z (2010), Palladium (II) and platinum (II) complexes of a symmetric Schiff base derived from 2,6, diformyl-4-methylphenol with N-aminopyrimidine: Synthesis, characterization and detection of DNA interaction by voltammetry. *European Journal of Medicinal Chemistry* 45, 4215–4220. https://doi.org/10.1016/j.ejmech.2010.06.016.

[12] Mocanu AS, Iliş M, Dumitraşcu F, Ilie M & Cîrcu V (2010), Synthesis, mesomorphism and luminescence properties of palladium (II) and platinum (II) complexes with dimeric Schiff base liquid crystals. *Inorganica Chimica Acta* 363: 729–736. https://doi.org/10.1016/j.ica.2009.11.028.

[13] Akbari A & Alinia Z (2013), Synthesis, characterization, and DFT calculation of a Pd (II) Schiff base complex. *Turkish Journal of Chemistry* 37, 867–878. https://doi.org/10.3906/kim-1207-74.

[14] Ruike RE, Kaasjager VE, Kliphuis D, Elsevier CJ, Van Leeuwen PWN, Vrieze K & Goubitz K (1996), Insertion Reactions Involving Palladium Complexes with Nitrogen Ligands. 2. Carbon monoxide and Alkene Insertion Reactions with Novel Palladium Compounds Containing Terdentate Ligands. *Organometallics* 15, 668–677. https://doi.org/10.1021/om9504361.

[15] Hauer CR, King GS, McCool EL, Euler WB, Ferrara JD & Youngs WJ (1987), Structure of 2,3-butanedione dihydrazone and IR study of higher polyazines: a new class of polymeric conductors. *Journal of the American Chemical Society* 109, 5760–5765. https://doi.org/10.1021/ja00253a031.

[16] Busch DH & Balier-Jr JC (1956), The Iron (II)-Methine Chromophore. *Journal of the American Chemical Society* 78, 1137–1142. https://doi.org/10.1021/ja01587a014.

[17] Chowdhury S, Drew MGB & Datta D (2003), A case of four-coordinate silver(I) adopting a high energy planar geometry. Experiment and theory. *New Journal of Chemistry* 27, 831–835. https://doi.org/10.1039/b211898j.

[18] Kesslen EC & Euler WB (1995), Synthesis and characterization of pyridine end-capped oligoazines. *Tetrahedron Letters* 36, 4725–4728. https://doi.org/10.1016/0040-4039(95)00888-J.

[19] Bariz R, Bremard C, Laureyns J & Merlin JC (1986), Raman and infrared spectroscopic studies of novel poly-aza chains. *Journal of Molecular Structure* 142, 439–442. https://doi.org/10.1016/0022-2860(86)85151-1.

[20] Geary WJ (1971), The use of conductivity measurements in organic solvents for the characterisation of coordination compounds. *Coordination Chemistry Reviews* 7, 81–122. https://doi.org/10.1016/S0010-8545(00)80009-0.

[21] Chakrabarty S, Nath B Ahmed A & Bhattacharjee S (2014), ICAIJ 9, 109.

[22] Chakrabarty S, Sarkhel P & Poddar RK (2010), Ruthenium (II) and palladium (II) complexes with 2, 6-(bispyrazol-1-yl) pyridines. *Journal of Co-ordination Chemistry* 63, 1563–1569. https://doi.org/10.1080/00958972.2010.482153.

[23] Lever ABP (1984), Inorganic Electronic Spectroscopy, 2nd Edn, Elsevier, Amsterdam.

[24] Frisch MJ, et al., (2009), Gaussian 09, Revision B.01, Gaussian Inc., Wallingford CT.

[25] Frisch E, Hratchian HP, Dennington II RD, Keith TA, Millam J, Nielsen B, Holder AJ & Hiscocks J (2009), Gaussian, Inc. GaussView Version 5.0.8, Wallinford, CT.

[26] Akbari A, Ahmadi M, Takjoo R & Heinemann FW (2013), X-ray structure and theoretical studies on a palladium (II) Schiff base complex. *Journal of Coordination Chemistry* 66, 1866–1875. https://doi.org/10.1080/00958972.2013.792334.

[27] Becke AD (1993), Density-functional thermochemistry. III. The role of exact exchange. *The Journal of Chemical Physics* 98(7), 5648–5652. https://doi.org/10.1063/1.464913.

[28] Lee C, Yang W & Parr RG (1988), Development of the Colle-Salvetti correlation energy formula into a functional of the electron density. *Physical Review B* 37(2), 785–789. https://doi.org/10.1103/PhysRevB.37.785.

[29] Drissi M, Benhalima N, Megrouss Y, Rahmani R, Chouaih A & Hamzaoui F (2015), Theoretical and Experimental Electrostatic Potential around the m-Nitrophenol Molecule. *Molecules* 20(3), 4042–4054. https://doi.org/10.3390/molecules20034042.

[30] Benaissi H, Drissi M, Yahiaoui S, Megrouss Y, Chouaih A & Hamzaoui F (2018), Hirshfeld surface analysis, topological features and nonlinear optical properties of phthalonitrile derivative: low temperature experimental charge density and quantum chemistry studies. *Journal of Optoelectronics and Biomedical Materials* 10(3), 73–82.

[31] Boukabcha N, Feddag A, Rahmani R, Chouaih A & Hamzaoui F (2018), Molecular structure, multipolar charge density study and nonlinear optical properties of 4-methyl-N-[(5-nitrothiophen-2-ylmethylidene)] aniline. *Journal of Optoelectronics and Advanced Materials* 20, 140–148.

[32] Boubegra N, Megrouss Y, Boukabcha N, Chouaih A & Hamzaoui F (2016), The electrostatic properties of 1,2-dimethyl-3-nitrobenzene compound: ab initio calculation and X-ray charge density analysis. *Rasayan Journal of Chemistry* 9, 751–761.

[33] Pulay P, Fogarasi G, Pongor G, Boggs JE & Vargha A (1983), Combination of theoretical ab initio and experimental information to obtain reliable harmonic force constants. Scaled quantum mechanical (QM) force fields for glyoxal, acrolein, butadiene, formaldehyde, and ethylene. *Journal of the American Chemical Society* 105, 7037–7047. https://doi.org/10.1021/ja00362a005.

[34] Johnson RD (2013), NIST Computational Chemistry Comparison and Benchmark Database NIST Standard Reference Database Number 101 Release 16a, Editor: Russell D. Johnson III, http://cccbdb.nist.gov/

[35] Wolinski K, Hinton JF & Pulay P (1990), efficient implementation of the gauge-independent atomic orbital method for NMR chemical shift calculations. *Journal of the American Chemical Society* 112, 8251–8260. https://doi.org/10.1021/ja00179a005.

[36] Bohmann JA, Weinhold F & Farrar TC (1997), Natural chemical shielding analysis of nuclear magnetic resonance shielding tensors from gauge-including atomic orbital calculations. *The Journal of Chemical Physics* 107, 1173–1184. https://doi.org/10.1063/1.474464.